

Stretchable Coplanar Self-Charging Power Textile with Resist-Dyeing Triboelectric Nanogenerators and Microsupercapacitors

Zifeng Cong,[#] Wenbin Guo,[#] Zihao Guo, Yanghui Chen, Mengmeng Liu, Tingting Hou, Xiong Pu,^{*} Weiguang Hu,^{*} and Zhong Lin Wang^{*}

Cite This: *ACS Nano* 2020, 14, 5590–5599

Read Online

ACCESS |

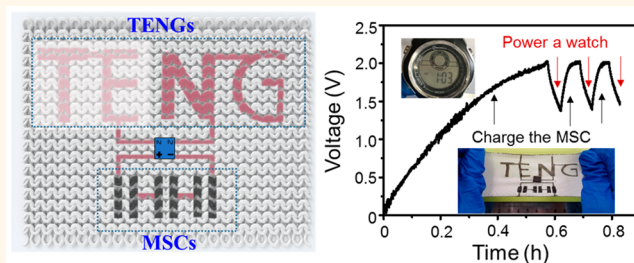
Metrics & More

Article Recommendations

Supporting Information

ABSTRACT: The integration between energy-harvesting and energy-storage devices into a self-charging power unit is an effective approach to address the energy bottleneck of wearable/portable/wireless smart devices. Herein, we demonstrate a stretchable coplanar self-charging power textile (SCPT) with triboelectric nanogenerators (TEGs) and microsupercapacitors (MSCs) both fabricated through a resist-dyeing-analogous method. The textile electrodes maintain excellent conductivity at 600% and 200% tensile strain along course and wale directions, respectively. The fabric in-plane MSC with reduced graphene oxides as active materials reaches a maximum areal capacitance of 50.6 mF cm^{-2} at 0.01 V s^{-1} and shows no significant degradation at 50% of tensile strain. The stretchable fabric-based TENG can output 49 V open-circuit voltage and 94.5 mW m^{-2} peak power density. Finally, a stretchable coplanar SCPT with one-batch resist-dyeing fabrication is demonstrated for powering small electronics intermittently without extra recharging. Our approach is also compatible with conventional textile processing and suggests great potential in electronic textiles and wearable electronics.

KEYWORDS: triboelectric nanogenerators, self-charging power textile, supercapacitors, stretchable, smart textile



Textile is an ideal platform for integrating with various functional electronic or optoelectronic devices for purposes ranging from health/sports monitoring, intelligent human/machine interfaces, and personal thermal management to fashion/aesthetics. Therefore, smart electronic textiles are widely pursued by both the industry and scientific communities with efforts from multidisciplinary fields. One of the long-lasting challenges is to provide electrical power supplies to these functional devices without sacrificing comfort, convenience, and fashion of a textile.^{1–4} State-of-the-art electrochemical energy storage devices, despite their great successes during the last decades in portable/wearable/wireless electronics, fall short mainly due to the following two aspects: limited flexibility and inconvenient frequent recharging. Therefore, flexible self-charging power textiles (SCPT), with integrated energy-harvesting and storage modules in a textile, have been recently studied,^{5–12} especially SCPTs integrated with fabric/yarn/fiber-based triboelectric nanogenerators (TENG).^{13–16} The electricity converted from human motions by the textile-based TENGs is *in situ* stored in the yarn/fabric-based energy storage devices, so as to elongate the operation time of electronics or even to eliminate the recharging and maintenance of conventional batteries.^{17–19} Hence, several

TENG-based SCPTs have been reported,^{15,20–26} some of which even been hybridized with solar cells.²⁷

Stretchability is almost inevitable for most textiles.²⁸ On one hand, it is mandatory throughout the fabrication courses of yarns and fabrics; on the other, it is required for comfortable experiences due to the unavoidable deformations caused by daily human body motions. For stretchable textile energy-storing supercapacitors or batteries, it is better to start with 2-D fabrics rather than 1-D fibers/yarns. Otherwise, the harsh deformations during the fabrication of a fabric can possibly damage the fiber/yarn-based supercapacitors/batteries. Coplanar textile-based supercapacitors/batteries, compared with the conventional stacked sandwich configuration, give better performance and can be fabricated with conventional textile printing or dyeing methods.^{29,30} For stretchable textile

Received: December 19, 2019

Accepted: May 5, 2020

Published: May 5, 2020



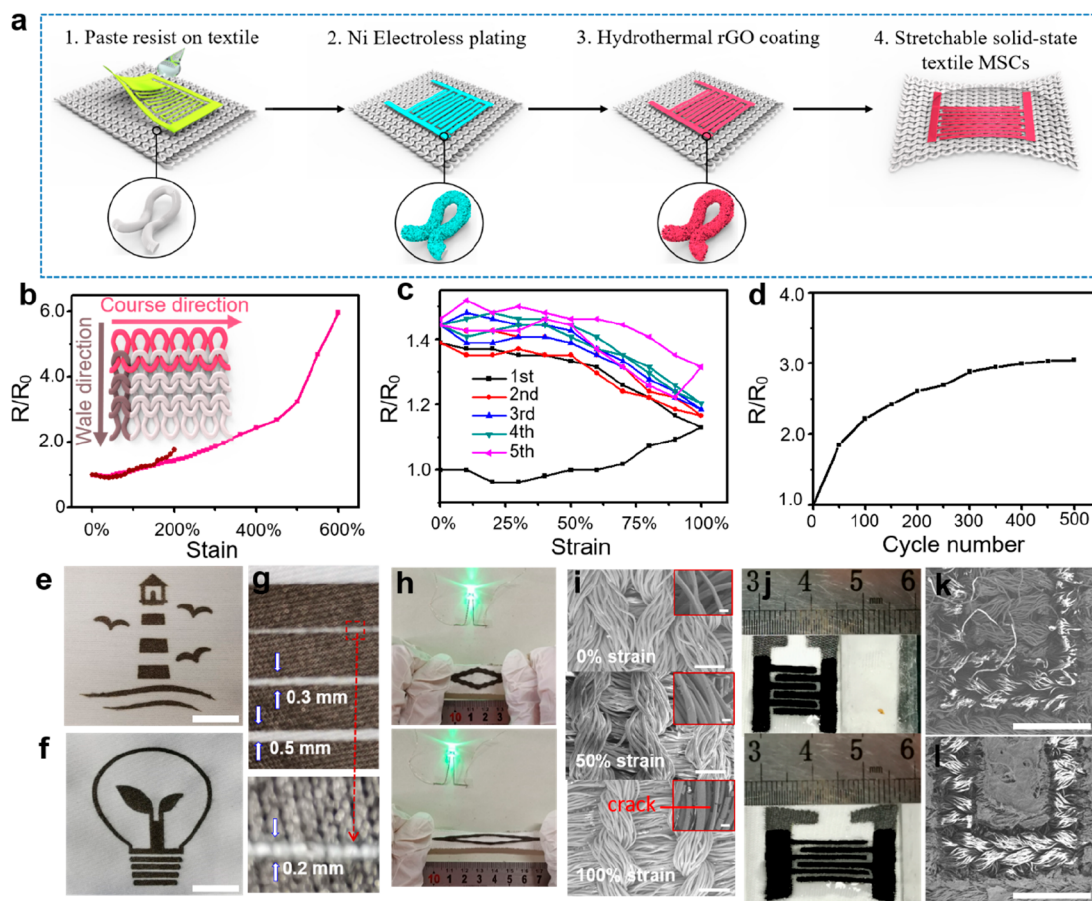


Figure 1. Resist-dyeing-analogous fabrication of stretchable textile conductors and MSCs. (a) Schematic illustration of the fabrication process. (b) Resistance variation of the Ni-coated textile conductors along course and wale directions (depicted top side of knit loops by the inset). Resistance variations during (c) the first five cycles and (d) prolonged 500 cycles of the textile conductors stretched between 0%–100% strain (course direction). (e, f) Photos of different conductive drawings fabricated on fabric substrates. (g) Conducting lines with different insulating gaps of 200, 300, and 500 μm . (h) Ni-coated textile used as conducting wire to light a LED at 0% strain (upper plot) and 100% strain (bottom plot). (i) SEM images of the knitting fibers at different tensile strains. (j) Photos of a textile MSC at original state (upper plot) and 50% stretched state (bottom plot). SEM images of a Ni-coated finger electrode on the fabric before (k) and after (l) the coating of rGO. The scale bar is 1 cm (e, f), 200 μm (i), 10 μm (insets in (i), 1 mm (k, l)).

TENGs, the key is to develop stretchable fiber-, yarn-, or fabric-based conductors sealed by dielectric polymers with compatible stretchability. Due to the absence of loose porous films for electrochemical reactions, either 1-D fibers/yarns or 2-D fabrics are feasible to start with. Several recent studies have demonstrated either yarn-based or fabric-based TENGs with excellent stretchability.^{31–33} 3D spacer fabric has also been applied on SCPT.^{34,35} Nevertheless, despite many reported stretchable fiber/fabric-based supercapacitors/batteries^{36–40} and stretchable textile TENGs, reports on stretchable integrated SCPTs is limited.⁴¹

Hence, a stretchable coplanar self-charging power textile is reported in this study with TENGs and microsupercapacitors (MSCs) integrated in one single knitted textile. A resist-dyeing-analogous method is developed to synthesize electrodes for these two modules. The electrodes maintain excellent conductivity at 600% tensile strain and 200% tensile strain along the course and wale direction, respectively. The solid-state MSC can reach a maximum areal capacitance of 50.6 mF cm^{-2} at 0.01 V s^{-1} and shows no significant degradation at 50% of tensile strain. Mechanical motions are demonstrated to be converted into electricity by the stretchable fabric-based TENG, which is then stored in the MSC modules for

intermittently powering small electronics without extra power supplies. The coplanar configuration of this SCPTs is also facile for aesthetic designs, and the fabrication is compatible with conventional textile processing routes.

RESULTS AND DISCUSSION

Figure 1a illustrates the fabrication procedure of the stretchable conductive textile and solid-state in-plane textile microsupercapacitors (MSC). A resist-dyeing-analogues method reported by us previously was utilized.⁴² The Kapton film with various patterns was attached on both sides of a knitted fabric (90% polyester, 10% Spandex) for serving as the resist. Electroless deposition of Ni coatings on the exposed textile was then carried out to obtain patterned conductive textile electrodes. Subsequently, rGO films were deposited onto the conductive textiles by a hydrothermal reduction of GO with Ni. A further hydrothermal reduction by ascorbic acid was conducted to further improve the conductivity of the rGO film. After detaching the Kapton resist, gel-type electrolyte (PVA-LiCl) was applied to achieve the solid-state textile MSCs. From our experience, this resist-dyeing method for patterned Ni conductive coatings works well for hydrophobic textile but not applicable for hydrophilic textile substrates (Figure S1).

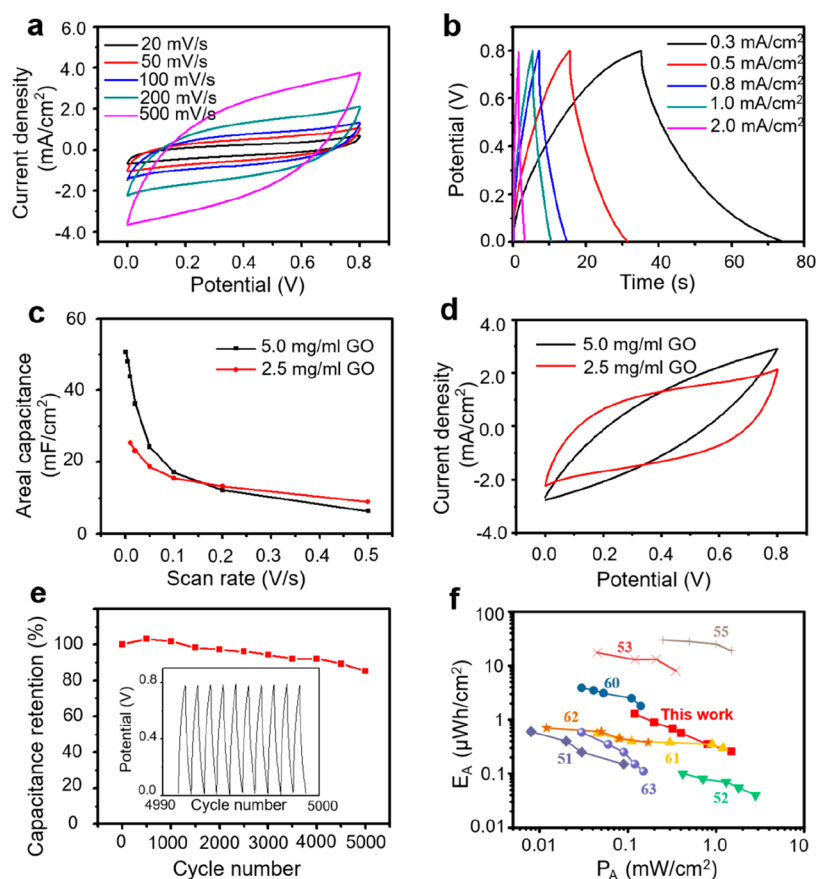


Figure 2. Electrochemical performances of the textile MSC. (a) Cyclic voltammetry (CV) and (b) galvanostatic charge/discharge (GCD) profiles of the MSC. (c) Variation of specific areal capacitances two MSCs with different rGO loadings. (d) CV profiles of the two MSCs at 0.2 V/s. (e) Cycling performance of the MSC at a current density of 2 mA cm⁻². The inset shows voltage profiles of the last 10 cycles. (f) Ragone plot of the textile MSC in comparison with other MSCs made of MWCNT/PANI on PET,⁶⁰ rGO/CNT on polyester,⁶¹ MnO₂ on paper,⁵¹ Ti₃C₂ MXene on paper,⁵² Graphite nanoflakes on polymer,⁶² Single-walled carbon nanotubes and polyaniline nanowires,⁶³ RuO₂/Ti₃C₂T_x on carbon fabric,⁵⁵ MnO₂/carbon nanotube composites on textile.⁵³

The Ni-coated textile is found to be an excellent stretchable conductor. The knitted fabric is known for its stretchability and elasticity. The weft-knitting loops are arranged by suspension in the horizontal (course) or vertical (wale) direction, as shown by the inset in Figure 1b. These meandering and suspended loops can be easily stretched in different directions so that they have more elasticity than other types of textiles. In uniaxial tensile test, the Ni-coated textile can be stretched to an ultimate strain of 650% and 260% along course and wale directions, respectively (see Figure S2a,c). It is noted that the Ni-coated textile, compared with the original bare textile, shows increased tensile strengths and elastic modulus with only slightly decreased ultimate tensile strain. The Ni-conductive fabric exhibited excellent conductivity (sheet resistance is 1.5 Ohm per square). The relative resistance R/R_0 of the Ni-coated textile is only about 1.12 at a tensile strain of 100% along either the course or wale direction (Figure 1b). It increases to 5.96 at 600% strain along the course direction and 1.76 at 200% strain along the wale direction. A detailed comparison with other state-of-the-art stretchable conductors is shown in Table S1.

The stability and durability of the textile conductor were assessed by measuring relative resistance when it was subjected to repetitive 100% of strain (Figure 1c,d). Figure 1c shows the resistance change during the first five stretching-releasing cycles (0–100% strain) along the course direction. For the

initial stretch below 30%, the resistance drops due to the decrease of contact resistances among joint fibers.⁴³ When the strain is larger than about 70%, the resistance increases, suggesting the gradually initiated cracks in the Ni coatings. Releasing the strain, the relative resistance keeps increasing to 1.39, but the resistance change is limited for the following four cycles. After 50 and 500 stretching–releasing cycles, the relative resistance increases to 1.91 and 3.05, respectively (see Figure 1d). For 50% stretching–releasing, the resistance increment is even smaller (Figure S3a). Similar trends are also observed along the wale direction (Figure S3a,b). The fabric fibers are loosely packed in knitting loops before stretching. These fibers will be tightened under tensile strain, which can lead to a decrease in contact resistance and an increase in conducting paths.^{44–46} Therefore, the resistance is first reduced. When the strain is further reduced, the relative rubbing motions among fibers can initiate cracks in the fibers, leading to the increase in the resistance. When the strain is high enough (about higher than 500% in the course direction, and 150% in the wale direction, as shown the Figure 1b), the fibers will deform and the metal coatings will be then damaged, resulting in the sharper increase in resistance. Therefore, the excellent conductivity at stretched states of the Ni textile is mainly originated from the knitting structures. If the strain is smaller than about 50%, the resistance of the textile can be quite stable since there is no damage in the Ni metal coatings.

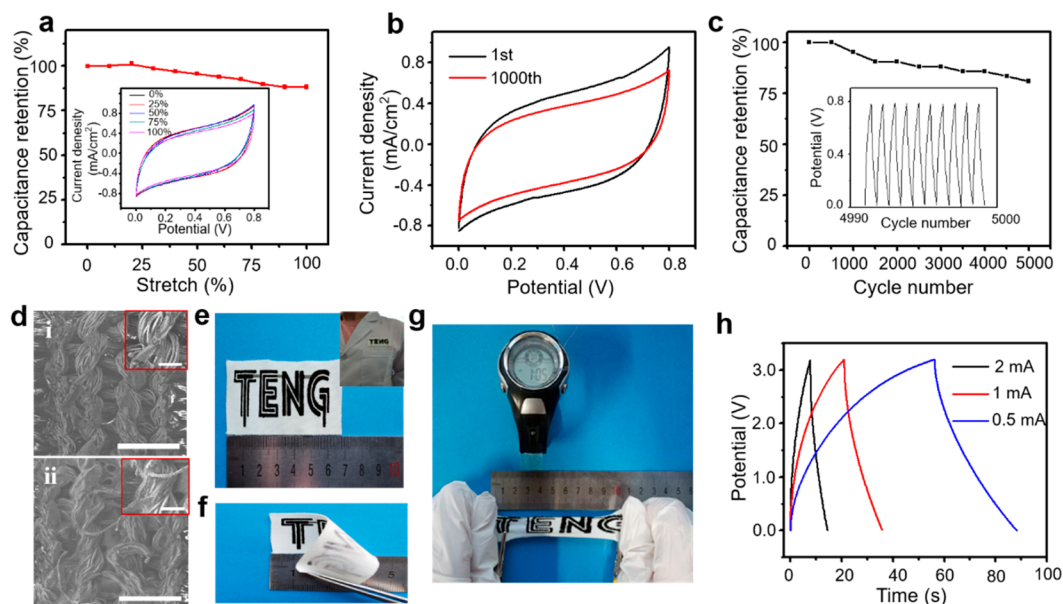


Figure 3. Stretchability and durability of the textile MSC. (a) Areal capacitance of the MSC at different strains (scan rate: 50 mV/s). The inset shows corresponding CV curves at various strains. (b) CV curves of the MSC after stretched 1000 cycles of 50% strain (scan rate: 50 mV/s). (c) Cycling performance of the MSC at 50% stretched state (current density of 2 mA cm⁻²). (d) SEM images of the rGO coatings without gel electrolyte (upper plot) and with gel electrolyte (bottom plot) after being 50% stretched for several times. (e) Photo of “TENG” letter-shaped MSCs in series connection. The inset shows a garment sewed with the MSCs. Photo of (f) the twisted MSCs and (g) a watch powered by the MSCs at 50% stretched state. (h) GCD curves of the letter-shaped MSCs at different currents.

One advantage of the resist-dyeing method is to make arbitrary conductive patterns on fabric, such as a demonstrated lighthouse (Figure 1e) and a light bulb (Figure 1f). The smallest feature size using this method is achieved to be 200 μm , as confirmed by conducting lines with different insulating gaps of 200, 300, and 500 μm in Figure 1g. Figure S1 shows that this resist-dyeing method is only applicable to relatively hydrophobic fabrics; otherwise, the deposition solutions may infiltrate into fibers underneath the Kapton resist. The hydrophobicity of the original textile is confirmed by the test of contact angle in Figure S4a,b. The Ni coatings are deposited only on the top layer fibers ($\sim 100 \mu\text{m}$ depth), not on the inside and backside fibers, as confirmed by the cross-sectional elemental mapping in Figure S5b–d. When the conducting textile pattern is used as the textile circuit, the brightness of a light-emitting diode (LED) does not change visibly after stretching (Figure 1h and video S1). Figure 1i shows the scanning electron microscopy (SEM) image of the Ni-coated knitted fabric at different tensile strains (0%, 50%, 100%). There is almost no cracks found in the Ni coatings at strain of 50%, but a few cracks are identified at strain of 100%, which is also consistent with resistance-strain trend in Figure 1c.

Figure 1j is a final solid-state stretchable textile MSC (with 1.0 mm wide finger electrode and 0.5 mm wide gap) at initial (upper plot) and 50% stretched state (bottom plot). Figure S6 shows the size of the stretchable textile MSCs. Figure 1k shows the SEM images of the Ni-coated knitted fabric, where a clear gap between finger electrodes can be observed and the knitted feature of the pristine fabric is maintained. After rGO coating, each finger electrode is uniformly covered with a layer of rGO (Figure 1l). The success of the reduction of GO is confirmed by X-ray diffraction (XRD) in Figure S7a and Raman spectra in Figure S7b. The XRD of final rGO film shows a broad peak at about 25° and the absence of the sharp peak of pristine GO

at around 10° ; the Raman spectroscopy of final rGO film exhibits a D to G band intensity ratio of $I_D/I_G > 1$.^{47,48}

Electrochemical performance of a stretchable textile MSC was measured with symmetric configuration using rGO films as double-layer capacitive materials in both electrodes and PVA/LiCl as a gel-type electrolyte. The cyclic voltammetry (CV) curves keep a slightly sloped rectangular shape even when the scanning rate is increased up to 0.5 V s⁻¹ (Figure 2a). The galvanostatic charge/discharge (GCD) curves at current densities ranging from 0.3 to 2 mA cm⁻² exhibited triangular shapes (Figure 2b), indicating the electrical double-layer capacitive behavior of the rGO active materials. The IR drop is 44, 70, and 115 mV at a current density of 0.3, 0.5, and 1 mA cm⁻², respectively, indicating a good electrical conductivity of the electrodes. The areal capacitance calculated by CV curves at 0.01 V s⁻¹ is 25.3 mF cm⁻², which maintains 8.8 mF cm⁻² at a scanning rate of 0.5 V s⁻¹ (Figure 2c). The capacitance value calculated from GCD curves is 14.5 mF cm⁻² at 0.2 mA cm⁻², which maintains 3.97 mF cm⁻² at 2 mA cm⁻² for 2.5 mg/mL sample; 32.5 mF cm⁻² at 0.5 mA cm⁻², which maintains 8.25 mF cm⁻² at 5 mA cm⁻² for a 5.0 mg/mL sample, as shown in Figure S8.

The areal loading of the rGO can be improved by increasing the concentration of GO solutions for hydrothermal depositions. By using 5 mg mL⁻¹ GO solution, the areal capacitance of high-loading textile MSC can reach 50.6 mF cm⁻² at 0.01 V s⁻¹ and maintains 17.1 mF cm⁻² at 0.1 V s⁻¹. Nevertheless, increasing the areal loading of rGO certainly degrades the rate capability and kinetics of MSC (Figure 2c,d) due to the elongated charge transfer lengths inside the electrodes. Detailed electrochemical performances of the textile MSC using 5 mg mL⁻¹ GO solution are shown in Figure S11. The textile MSCs also show stable cycling performances, achieving a capacitance retention of 85.3% after charging/discharging at 2.0 mA cm⁻² for 5000 cycles

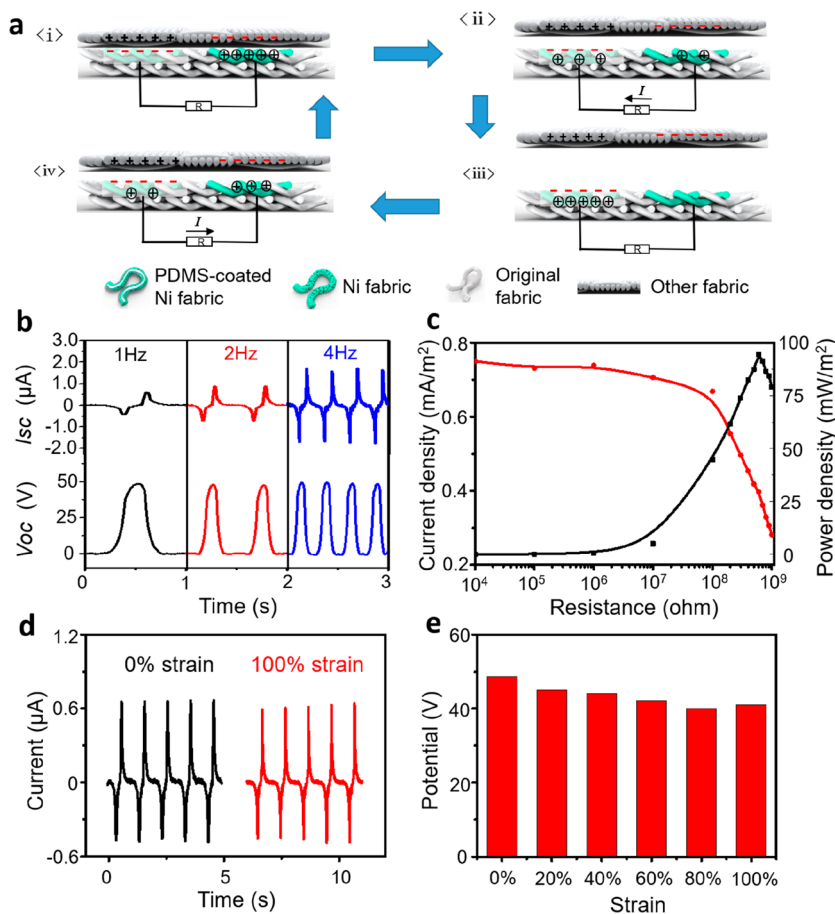


Figure 4. Stretchable textile TENGs. (a) Scheme of the working mechanism of the coplanar TENG. (b) I_{sc} and V_{oc} at various motion frequencies. (c) Variation of the output current density and power density with the external loading resistance. (d) I_{sc} of the stretchable TENG at tensile strains of 0% and 100%. (e) V_{oc} of the stretchable TENG at different strains.

(Figure 2e). The charging/discharging profiles kept the triangular shape during the course of the cycling and showed no significant degradation (the inset in Figure 2e). It is interesting to note that the capacitance increases in the first 1000 cycles. This phenomenon might be due to the coverage of the electrode by the gel electrolyte. It is ascribed to the slow wetting of the rGO with PVA-gel electrolyte because of the hydrophobic characteristic of rGO.^{49,50}

Energy density and power density of the textile MSCs are summarized in Figure 2f. The areal energy density of stretchable textile MSC was estimated to be 0.35–1.3 $\mu\text{Wh cm}^{-2}$. The areal energy density is higher than paper-based MSCs, e.g., MnO_2 on paper (0.6 $\mu\text{Wh cm}^{-2}$)⁵¹ and Ti_3C_2 MXene on paper (0.1 $\mu\text{Wh cm}^{-2}$),⁵² due to the larger surface area of porous textiles. Comparing with other reported textile MSCs with pseudocapacitive species, our areal energy density is smaller, e.g., MnO_2 /carbon nanotube composites (17.5 $\mu\text{Wh cm}^{-2}$),⁵³ MWNT/ V_2O_5 (3.31 $\mu\text{Wh cm}^{-2}$),⁵⁴ and RuO_2 / $\text{Ti}_3\text{C}_2\text{T}_x$ (19 $\mu\text{Wh cm}^{-2}$).⁵⁵ In addition, some reported that the dip-coating or screen-printing methods can load more active materials and therefore higher areal energy density, as summarized more detailed comparison with other state-of-the-art textile MSCs in Table S2. The areal power density of our stretchable textile MSC can reach 1.5 mW cm^{-2} , generally comparable with MSCs in Table S2. The high power density is mainly due to the high conductivity of the Ni coating, large surface area of the rGO, and little interfacial contact resistance

between the electrode and gel electrolyte, as shown in Figure S9.

The stretchability and durability of the textile MSCs were also examined. Figure 3a shows the areal capacitance of a textile MSC at various strains from 0% to 100% (along course direction) obtained from CV curves at 0.05 V s^{-1} . The capacitance at a strain of 50% and 100% is maintained to be 95.0% and 88.2% of that at the initial state, respectively. No significant degradation in CV curves is found for the textile MSC at stretched states (Figure 3a, inset). After 1000 cycles of stretching–releasing to 50% of strain, the capacitance retention based on the CV test remains at 85.0% (Figure 3b). The capacitance retention tested at the 50% stretched state remains 80.9% after 5000 cycles of galvanostatic charging/discharging (Figure 3c and the inset), which is only slightly smaller than that obtained at the unstrained state (Figure 2e). The excellent stretchability and durability of the textile MSC are mainly due to the following two aspects: first, the current collector (i.e., Ni-coated fabrics) is highly stretchable and durable as discussed in Figure 1. Second, elastomeric PVA hydrogel served as a binder to enhance the binding forces at the interfaces between rGO and conductive fiber.⁵⁶ The active rGO film, infiltrated with hydrogel, is converted into an elastomeric composite film, which can accommodate to the tensile strain without mechanical degradation.⁵⁷ As confirmed in Figure 3d, cracks are found in the rGO films on the fibers at 50% of strain when there is no gel electrolyte (upper image); in contrast, no crack

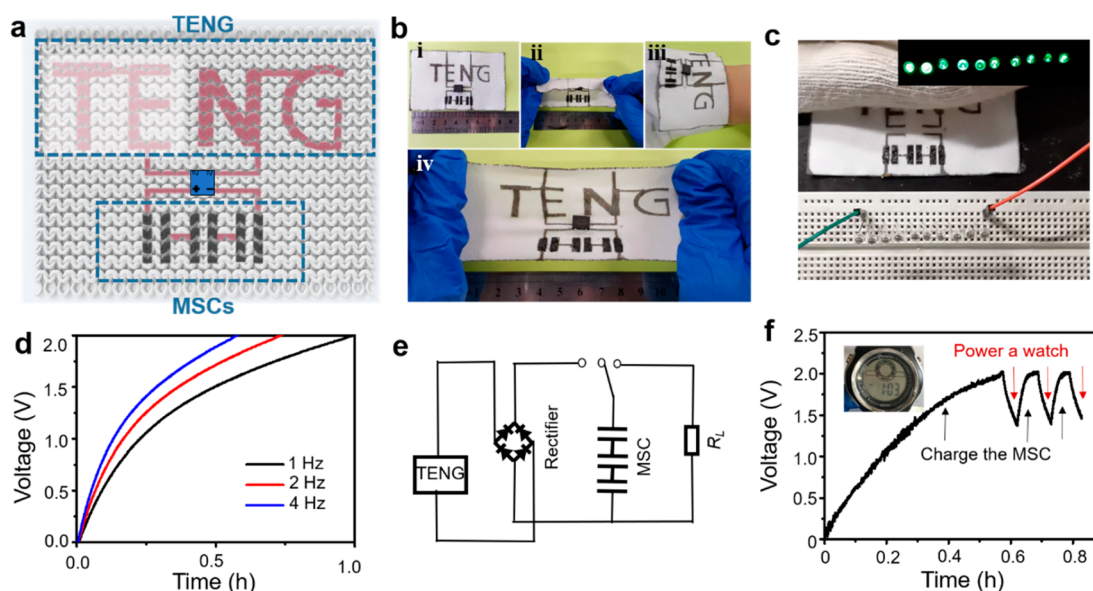


Figure 5. Stretchable coplanar self-charging power textile. (a) Schematic illustration of the coplanar SCPT by integrating a letter-shaped TENG and three series-connected MSCs in a common fabric. (b) Photos of a SCPT (i, ii, iii) sewn in a garment and at 50% of tensile strain (iv). (c) 10 LEDs lighted up by hand tapping the fabric TENG. (d) Voltage profile of the MSCs charged by the TENG fabrics at different motion frequencies. (e) Equivalent circuit of the SCPT. (f) Voltage profile of the three series-connected MSCs charged by the coplanar TENG fabrics and discharged by powering an electronic watch (inset photo).

is observed after the gel electrolyte is applied (bottom image). Bending and twisting performance were also measured, as shown in Figure S10, and there is no significant capacitance degradation under bending and twisting conditions.

A comfortable, aesthetic, or stylish design is also required for textile power devices. With the resist-dyeing-analogous method, arbitrary-shaped logos or patterns in a fabric can be converted into an energy-storage MSC. For demonstration, four MSCs were designed on a knitted fabric in the form of four letters, *i.e.*, “TENG,” as shown in Figure 3e,f. Each letter is composed of two rGO electrodes. The Ni textile lines are used to connect adjacent letter for series connection without using extra wires. Solid electrolyte was covered on each MSC separately. The “TENG” MSC obtained a voltage up to 3.2 V and discharge capacitances of 5.0, 4.9, 4.2 mF at a galvanostatic discharging current of 0.5, 1.0, 2.0 mA, respectively (Figure 3h). This textile-based planar MSC can power a watch at a strain of 50% after being charged (Figure 3g). More complicated letters or images could also be designed into stretchable and aesthetic energy-storing textiles, as long as appropriate resist is designed.

A stretchable textile TENG was developed with the resist-dyeing-analogous method as well, using Ni-coated textile as two in-plane electrodes. An elastomeric PDMS thin layer was coated on the top of only one of the electrodes. The working mechanism of the stretchable fabric TENG is schematically demonstrated in Figure 4a. When a polyester textile is in contact with the TENG textile, contact electrification occurs at the PDMS–polyester interfaces, generating net negative charges in the PDMS and positive charges in the polyester due to the contact electrification effect; similarly, the polyester fabrics will be negatively charged and the Ni-coated fabrics will be positively charged at the polyester–Ni interfaces (Figure 4a(i)). When the polyester fabric is gradually separating away from the TENG textile, the unbalanced positive charges in the Ni fabric will flow through the external circuit to arrive at the other Ni-textile electrodes, so as to screen the static charges in

the PDMS (Figure 4a(ii)). The current flow stops when all of the static charges are screened and equilibrium is achieved (Figure 4a(iii)). If the counter polyester textile is approaching back to contact the TENG textile, a reversed current flow in the external circuit is generated until local charge equilibrium is achieved again (Figure 4a(iv)). The repeated touching-separating motions are then converted into pulsed alternative current (AC).

A linear motor was used to provide contact-separation movement between a polyester fabric and the TENG-textile. The contact area is fixed to be $4 \times 2 \text{ cm}^2$. Figure 4b shows the t short-circuit current (I_{sc}) and open-circuit voltage (V_{oc}) of the fabric TENG under various motion frequencies (1, 2, and 4 Hz). The V_{oc} (and Q_{sc}) is stable at $\sim 49 \text{ V}$ (and 28 nC) and independent of frequency, while the I_{sc} increases with the frequency from $\sim 0.6 \mu\text{A}$ at 1 Hz to $\sim 1.8 \mu\text{A}$ at 4 Hz (Figure 4b and Figure S12b). A maximum output areal power density was measured to be $\sim 94.5 \text{ mW m}^{-2}$ at a matched resistance of $\sim 500 \text{ megaOhm}$. The stability of the fabric TENG is confirmed by measuring about 5000 cycles of repeated current output at 1 Hz motion, showing no obvious degradation in Figure S13. The fabric TENG is stretchable as both electrodes and electrification layers are stretchable. After being stretched for 100% strain along the course direction, there is no significant decrease in the I_{sc} (Figure 4d). The V_{oc} measured at different strains are shown in Figure 4e, exhibiting a slight decrease from 49 to 41 V at 100% strain. The impact of humidity was investigated in Figure S14, including the long-term performance in a humid environment. It can be observed that the output increases in dry environment (20% relative humidity) and decrease in the humid environment (50% relative humidity). The output voltage also fluctuates in humid environment for long-term test. Nevertheless, these data also demonstrate the textile TENG can work in a humid environment, but future research is still required to avoid the negative effect of humidity and human sweat.^{58,59}

Considering the two in-plane configurations of the TENG textile and MSC textile, it is feasible to develop a self-charging power textile by combining the energy-harvesting and energy-storage modules in one single fabric. Therefore, one single Kapton resist was designed for fabricating electrodes of the TENG and MSC through a one-batch resist-dyeing process. Figure 5a shows a schematic layout of the self-charging power textile, consisting of a “TENG”-shaped TENG textile, a rectifier, and three MSCs connected in series. A PDMS layer is coated only on the Ni-coated “TE” letter-shaped electrode, which serves as the PDMS coated Ni fabric in Figure 4a; the “NG” electrode without PDMS coating serves as the uncoated Ni fabric in Figure 4a. Then, electricity can be generated by the “TENG” letter-shaped TENG textile when in contact with the other textiles. All of the electrical connections are made of Ni-conductive lines coated on the fabric without any other wires. The pins of the rectifier are sewn and soldered on the conductive fabric lines for better anchoring. A photo of the final self-charging power textile is shown in Figure 5b(i), which is soft (Figure 5b(ii)) and can be directly sewn on a common cloth (Figure 5b(iii)). It can be easily stretched for about 50% strain without any damage (Figure 5b(iv)). By tapping the “TENG” textile with a polyester glove, 10 green LEDs can be easily lighted (Figure 5c and video S2). After 100 cycles of 50% stretching, the I_{sc} and V_{oc} only showed slight decrement by hand tapping at roughly about 4 Hz (hand tapping with the aid of a metronome APP in a cell phone, Figure S15a,b). The stability of the TENG textile was further confirmed by the rectified current recorded at a 50% stretched state for more than 1 h of tapping by a linear motor at 1 Hz (Figure S15c). Figure S16 shows the GCD curves at 1 mA charging/discharging current of stretchable coplanar MSCs at original state and after 100 cycles of 50% stretching. The series-connected three MSCs can reach a voltage of 2.4 V and a capacitance of 2.1 mF, which kept to be 1.82 mF after 100 cycles of stretching.

The self-charging power textile was charged by tapping the TENG fabric with a polyester fabric at different frequencies using a linear motor and the voltages of the MSCs were recorded in Figure 5d. It took about 56, 43, and 35 min to reach 2.0 V for 1, 2, and 4 Hz motions, respectively. The equivalent circuit of the self-charging power textile is shown in Figure 5e. After charging to 2.0 V by 34 min of 4 Hz tapping with a linear motor, the self-charging power textile can be used to power an electronic watch (inset in Figure 5f) for 3 min and the voltage of MSCs drop to 1.4 V. Subsequently, 4.2 and 3.6 min of charging back to 2.0 V can provide the power supply for the watch for 2.5 and 2.4 min, respectively (Figure 5f). These results confirmed that the self-charging power textile can be applied as a textile power source for providing electricity intermittently and independently to small wearable electronics without extra power devices.

CONCLUSIONS

In summary, we demonstrated a stretchable coplanar self-charging power textile (SCPT) with energy-harvesting triboelectric nanogenerators and energy-storage microsupercapacitors both fabricated through a resist-dyeing-analogous method. The fabricated conductive electrodes showed excellent stretchability, which can be stretched up to 600% and 200% along course and wale directions in resistance test, respectively. Even after 500 cycles of 100% stretch, the resistance of the textile electrodes showed no significant increase. The solid-

state MSC with rGO as capacitive active materials could reach a maximum areal capacitance of 50.6 mF cm⁻² and showed no significant degradation at 50% of tensile strain as well. The stretchable fabric-based TENG can output 49 V open-circuit voltage and 94.5 mW m⁻² peak power density. Finally, a stretchable coplanar SCPT with one-batch resist-dyeing fabrication was demonstrated for powering small electronics. Considering the demonstrated excellent stretchability and compatibility with conventional textile processing routes of the SCPT, our approach to energy textile promises great potential in electronic textiles and wearable electronics, but future research is still required to address the washability issues of energy storage textiles and the integrated self-charging power textiles.

METHODS

Fabrication of Stretchable Ni-Coated Textile. First, the stretchable fabric (75D double sided purchased from Zhong Shi Textile) with a thickness of 0.53 mm was cleaned with ethanol, acetone, and distilled water in an ultrasonic bath for 30 min for 5 times. Subsequently, commercial Kapton was used to cover both sides of the textile tightly. The resist patterns were cut on the textile using laser cutting only cutting through the Kapton resist. The resist-covered textile was sensitized by aqueous solution with 10 g L⁻¹ SnCl₂ and 0.5 g L⁻¹ PdCl₂, and finally immersed in an aqueous solution containing 0.1 M NiSO₄·6H₂O, 0.3 M NaH₂PO₄·H₂O, 0.05 M C₆H₅Na₃O₇·2H₂O, 0.5 M H₃BO₃ for 24 h at room temperature. After washing and drying the textile, the Kapton resist was detached and patterned conductive textile was obtained. The resistance of Ni-coated and rGO-Ni-coated fabric (both with a width of 0.5 cm) is 2.6 Ohm/cm and 4.5 Ohm/cm, which were measured using multimeter.

Fabrication of Solid-State Microsupercapacitors. The Ni-coated textile was immersed in a 2.5 mg mL⁻¹ GO dispersion for hydrothermal reaction at 80 °C for 6 h. Then the rGO-coated Ni textile was soaked in a 0.1 M ascorbic acid at 80 °C for 1 h for further reduction of coated rGO. The thickness of the pristine fabric is 0.530 mm and 0.650 mm after Ni coating. After coating rGO in 2.5 mg mL⁻¹ GO suspensions, the thickness increases to 0.716 mm. Finally, the obtained rGO-Ni-fabric was washed with DI water and dried in vacuum oven. For the gel electrolyte, 4 g PVA (M_w 89 000–98 000) was added into 40 mL of 2 M LiCl solution and then stirred at 90 °C for 2 h. Subsequently, the textile based MSC was immersed in the PVA-LiCl solid electrolyte for 5 min and solidified at 50 °C for 1 h. Another sample with 5.0 mg mL⁻¹ GO dispersion for hydrothermal reaction was also conducted with the same procedures. The areal loading for 2.5 and 5 mg mL⁻¹ samples is 1.1 and 2.4 mg cm⁻², respectively.

Fabrication of the Coplanar Self-Charging Power Textile. All of the electrodes and connecting lines were fabricated with one Kapton resist. A Ni-coated “TE” letter-shaped electrode was then immersed in a mixture of Sylgard 184 base and cross-linker (10:1 by weight) for 10 min and then dried in vacuum oven at 70 °C for 2 h. The rectifier (SOP-4 purchased from Shenzhen Tongsheng electronic) was sewn and soldered in Ni-coated fabric between TENG and MSCs. LED (F5 purchased from Shanghai Hongcheng Electronic).

Characterization. The electrochemical performance was measured by an electrochemical workstation (CHI 660E). The output short current and open-circuit voltage of the TENG cloth were measured by a Keithley electrometer (Keithley 6514). A 4-point probe system (RTS-9) was used to measure the square resistance. Five regions were also randomly selected for measurement, and the mean value was calculated. XRD measurements were measured by a Panalytical instrument (X'Pert 3 Powder). Raman spectra were performed with a confocal Raman spectrometer (HORIBA LabRAM HR Evolution). SEM was taken with a Hitachi SU8200. The capacitance was calculated from CV and GCD profiles respectively by

$$C_{\text{device}} = \frac{\int_0^U i(u) du}{vU} \quad (1)$$

$$C_{\text{device}} = \frac{It}{U} \quad (2)$$

where I is the discharging current, t is the discharging time, U is the cutoff voltage (i.e., 0.8 V), v is the scanning rate. Areal specific capacitance (CA) according to the following formula

$$C_A = \frac{C_{\text{device}}}{A} \quad (3)$$

where A is the area of the device measured to be about 1.58 cm². The areal energy density and power density were obtained by

$$E_A = \frac{1}{2} \times C_A \times \frac{U^2}{3600} \quad (4)$$

$$P_A = \frac{3600 \times E_A}{t} \quad (5)$$

where t is the discharging time calculated from discharging curves.

ASSOCIATED CONTENT

Supporting Information

The Supporting Information is available free of charge at <https://pubs.acs.org/doi/10.1021/acsnano.9b09994>.

Resist dyeing coating of other fabrics; uniaxial tensile test of the original textile and Ni-coated textile at course and wale direction; cycle performance of the Ni-coated textile during 50 stretching-releasing cycles (0–50% strain) along course direction and wale direction and resistance change of the Ni-coated textile during the first stretching-releasing cycle (0–100% strain) along wale direction; contact angle measurements of original textile and Ni-coated textile; cross-sectional scanning electron microscopy (SEM) images and energy dispersive X-ray spectroscopy (EDS) elemental mapping of a Ni-coated fabric; the dimensions of the textile stretchable MSC; X-ray diffraction and Raman spectra of the GO and rGO; the specific areal capacitances with different current density; Nyquist plots of the textile MSC at 0% strain and 50% strain; bending and twisting performance; electrochemical behavior of the textile MSC using 5 mg mL⁻¹ GO solution; the Q_{SC} of the textile TENG at 0% strain and 100% strain; current output stability of the coplanar power textile; performance of the TENG in humidity environment; the I_{SC} and V_{OC} of TENG textile after stretched 100 cycles of 50% strain by hand tapping; GCD curves of coplanar and stretchable MSCs after stretched 100 cycles (PDF)

Movie S1: Stretchability of the conductive Ni-coated textile (AVI)

Movie S2: Lighting 10 green LEDs by tapping the TENG textile (AVI)

AUTHOR INFORMATION

Corresponding Authors

Xiong Pu – CAS Center for Excellence in Nanoscience, Beijing Key Laboratory of Micro-Nano Energy and Sensor, Beijing Institute of Nanoenergy and Nanosystems, Chinese Academy of Sciences, Beijing 100083, China; School of Nanoscience and Technology, University of Chinese Academy of Sciences, Beijing 100049, China; Center on Nanoenergy Research, School of Chemistry and Chemical Engineering, School of Physical Science

and Technology, Guangxi University, Nanning 530004, China; orcid.org/0000-0002-1254-8503; Email: puxiong@binn.cas.cn

Weiguo Hu – CAS Center for Excellence in Nanoscience, Beijing Key Laboratory of Micro-Nano Energy and Sensor, Beijing Institute of Nanoenergy and Nanosystems, Chinese Academy of Sciences, Beijing 100083, China; School of Nanoscience and Technology, University of Chinese Academy of Sciences, Beijing 100049, China; Center on Nanoenergy Research, School of Chemistry and Chemical Engineering, School of Physical Science and Technology, Guangxi University, Nanning 530004, China; orcid.org/0000-0002-8614-0359; Email: huweiguo@binn.cas.cn

Zhong Lin Wang – CAS Center for Excellence in Nanoscience, Beijing Key Laboratory of Micro-Nano Energy and Sensor, Beijing Institute of Nanoenergy and Nanosystems, Chinese Academy of Sciences, Beijing 100083, China; School of Nanoscience and Technology, University of Chinese Academy of Sciences, Beijing 100049, China; Center on Nanoenergy Research, School of Chemistry and Chemical Engineering, School of Physical Science and Technology, Guangxi University, Nanning 530004, China; School of Materials Science and Engineering, Georgia Institute of Technology, Atlanta, Georgia 30332-0245, United States; orcid.org/0000-0002-5530-0380; Email: zlwang@gatech.edu

Authors

Zifeng Cong – CAS Center for Excellence in Nanoscience, Beijing Key Laboratory of Micro-Nano Energy and Sensor, Beijing Institute of Nanoenergy and Nanosystems, Chinese Academy of Sciences, Beijing 100083, China; School of Nanoscience and Technology, University of Chinese Academy of Sciences, Beijing 100049, China

Wenbin Guo – CAS Center for Excellence in Nanoscience, Beijing Key Laboratory of Micro-Nano Energy and Sensor, Beijing Institute of Nanoenergy and Nanosystems, Chinese Academy of Sciences, Beijing 100083, China; School of Nanoscience and Technology, University of Chinese Academy of Sciences, Beijing 100049, China

Zihao Guo – CAS Center for Excellence in Nanoscience, Beijing Key Laboratory of Micro-Nano Energy and Sensor, Beijing Institute of Nanoenergy and Nanosystems, Chinese Academy of Sciences, Beijing 100083, China; School of Nanoscience and Technology, University of Chinese Academy of Sciences, Beijing 100049, China

Yanghui Chen – CAS Center for Excellence in Nanoscience, Beijing Key Laboratory of Micro-Nano Energy and Sensor, Beijing Institute of Nanoenergy and Nanosystems, Chinese Academy of Sciences, Beijing 100083, China; School of Nanoscience and Technology, University of Chinese Academy of Sciences, Beijing 100049, China

Mengmeng Liu – CAS Center for Excellence in Nanoscience, Beijing Key Laboratory of Micro-Nano Energy and Sensor, Beijing Institute of Nanoenergy and Nanosystems, Chinese Academy of Sciences, Beijing 100083, China; School of Nanoscience and Technology, University of Chinese Academy of Sciences, Beijing 100049, China

Tingting Hou – CAS Center for Excellence in Nanoscience, Beijing Key Laboratory of Micro-Nano Energy and Sensor, Beijing Institute of Nanoenergy and Nanosystems, Chinese Academy of Sciences, Beijing 100083, China; School of Nanoscience and Technology, University of Chinese Academy of Sciences, Beijing 100049, China

Complete contact information is available at:
<https://pubs.acs.org/10.1021/acsnano.9b09994>

Author Contributions

#Z.F.C. and W.B.G. contributed equally to this work.

Notes

The authors declare no competing financial interest.

ACKNOWLEDGMENTS

The authors thank for the support from the Youth Innovation Promotion Association of CAS, National Key Research and Development Program of China (2016YFA0202703), National Natural Science Foundation of China (Grant Nos. 51432005, 61574018, and 51603013), and “Hundred Talents Program” of CAS.

REFERENCES

- (1) Shi, J.; Liu, S.; Zhang, L.; Yang, B.; Shu, L.; Yang, Y.; Ren, M.; Wang, Y.; Chen, J.; Chen, W.; Chai, Y.; Tao, X. Smart Textile-Integrated Microelectronic Systems for Wearable Applications. *Adv. Mater.* **2020**, *32*, 1901958.
- (2) Stoppa, M.; Chiolerio, A. Wearable Electronics and Smart Textiles: A Critical Review. *Sensors* **2014**, *14*, 11957–11992.
- (3) Sun, H.; Zhang, Y.; Zhang, J.; Sun, X.; Peng, H. Energy Harvesting and Storage in 1D Devices. *Nat. Rev. Mater.* **2017**, *2*, 17023.
- (4) Wang, L.; Fu, X.; He, J.; Shi, X.; Chen, T.; Chen, P.; Wang, B.; Peng, H. Application Challenges in Fiber and Textile Electronics. *Adv. Mater.* **2020**, *32*, 1901971.
- (5) Kwak, S. S.; Yoon, H.-J.; Kim, S.-W. Textile-Based Triboelectric Nanogenerators for Self-Powered Wearable Electronics. *Adv. Funct. Mater.* **2019**, *29*, 1804533.
- (6) Yang, Z.; Deng, J.; Sun, H.; Ren, J.; Pan, S.; Peng, H. Self-Powered Energy Fiber: Energy Conversion in the Sheath and Storage in the Core. *Adv. Mater.* **2014**, *26*, 7038–7042.
- (7) Jiang, Q.; Wu, C.; Wang, Z.; Wang, A. C.; He, J.-H.; Wang, Z. L.; Alshareef, H. N. MXene Electrochemical Microsupercapacitor Integrated with Triboelectric Nanogenerator as a Wearable Self-Charging Power Unit. *Nano Energy* **2018**, *45*, 266–272.
- (8) Chai, Z.; Zhang, N.; Sun, P.; Huang, Y.; Zhao, C.; Fan, H. J.; Fan, X.; Mai, W. Tailorable and Wearable Textile Devices for Solar Energy Harvesting and Simultaneous Storage. *ACS Nano* **2016**, *10*, 9201–9207.
- (9) Chen, J.; Huang, Y.; Zhang, N.; Zou, H.; Liu, R.; Tao, C.; Fan, X.; Wang, Z. L. Micro-Cable Structured Textile for Simultaneously Harvesting Solar and Mechanical Energy. *Nat. Energy* **2016**, *1*, 16138.
- (10) Pu, X.; Hu, W.; Wang, Z. L. Toward Wearable Self-Charging Power Systems: The Integration of Energy-Harvesting and Storage Devices. *Small* **2018**, *14*, 1702817.
- (11) Sun, P.; Qiu, M.; Li, M.; Mai, W.; Cui, G.; Tong, Y. Stretchable Ni@NiCoP Textile for Wearable Energy Storage Clothes. *Nano Energy* **2019**, *55*, 506–515.
- (12) Gao, Z.; Liu, P.; Fu, X.; Xu, L.; Zuo, Y.; Zhang, B.; Sun, X.; Peng, H. Flexible Self-Powered Textile Formed by Bridging Photoactive and Electrochemically Active Fiber Electrodes. *J. Mater. Chem. A* **2019**, *7*, 14447–14454.
- (13) Pu, X.; Li, L.; Liu, M.; Jiang, C.; Du, C.; Zhao, Z.; Hu, W.; Wang, Z. L. Wearable Self-Charging Power Textile Based on Flexible Yarn Supercapacitors and Fabric Nanogenerators. *Adv. Mater.* **2016**, *28*, 98–105.
- (14) Wen, Z.; Yeh, M.-H.; Guo, H.; Wang, J.; Zi, Y.; Xu, W.; Deng, J.; Zhu, L.; Wang, X.; Hu, C.; Zhu, L.; Sun, X.; Wang, Z. L. Self-Powered Textile for Wearable Electronics by Hybridizing Fiber-Shaped Nanogenerators, Solar Cells, and Supercapacitors. *Sci. Adv.* **2016**, *2*, 1600097.
- (15) He, T.; Wang, H.; Wang, J.; Tian, X.; Wen, F.; Shi, Q.; Ho, J. S.; Lee, C. Self-Sustainable Wearable Textile Nano-Energy Nano-System (NENS) for Next-Generation Healthcare Applications. *Adv. Sci.* **2019**, *6*, 1901437.
- (16) Lin, Z.; Yang, J.; Li, X.; Wu, Y.; Wei, W.; Liu, J.; Chen, J.; Yang, J. Large-Scale and Washable Smart Textiles Based on Triboelectric Nanogenerator Arrays for Self-Powered Sleeping Monitoring. *Adv. Funct. Mater.* **2018**, *28*, 1704112.
- (17) Hinchet, R.; Yoon, H.-J.; Ryu, H.; Kim, M.-K.; Choi, E.-K.; Kim, D.-S.; Kim, S.-W. Transcutaneous Ultrasound Energy Harvesting Using Capacitive Triboelectric Technology. *Science* **2019**, *365*, 491–494.
- (18) Kwak, S. S.; Kim, S.; Ryu, H.; Kim, J.; Khan, U.; Yoon, H.-J.; Jeong, Y. H.; Kim, S.-W. Butylated Melamine Formaldehyde as a Durable and Highly Positive Friction Layer for Stable, High Output Triboelectric Nanogenerators. *Energy Environ. Sci.* **2019**, *12*, 3156–3163.
- (19) Khan, U.; Kim, T. H.; Ryu, H.; Seung, W.; Kim, S. W. Graphene Tribotronics for Electronic Skin and Touch Screen Applications. *Adv. Mater.* **2017**, *29*, 201603544.
- (20) Chen, J.; Guo, H.; Pu, X.; Wang, X.; Xi, Y.; Hu, C. Traditional Weaving Craft for One-Piece Self-Charging Power Textile for Wearable Electronics. *Nano Energy* **2018**, *50*, 536–543.
- (21) Yang, Y.; Xie, L.; Wen, Z.; Chen, C.; Chen, X.; Wei, A.; Cheng, P.; Xie, X.; Sun, X. Coaxial Triboelectric Nanogenerator and Supercapacitor Fiber-Based Self-Charging Power Fabric. *ACS Appl. Mater. Interfaces* **2018**, *10*, 42356–42362.
- (22) Seung, W.; Gupta, M. K.; Lee, K. Y.; Shin, K.-S.; Lee, J.-H.; Kim, T. Y.; Kim, S.; Lin, J.; Kim, J. H.; Kim, S.-W. Nanopatterned Textile-Based Wearable Triboelectric Nanogenerator. *ACS Nano* **2015**, *9*, 3501–3509.
- (23) Dudem, B.; Mule, A. R.; Patnam, H. R.; Yu, J. S. Wearable and Durable Triboelectric Nanogenerators via Polyaniline Coated Cotton Textiles as a Movement Sensor and Self-Powered System. *Nano Energy* **2019**, *55*, 305–315.
- (24) Song, Y.; Zhang, J.; Guo, H.; Chen, X.; Su, Z.; Chen, H.; Cheng, X.; Zhang, H. All-Fabric-Based Wearable Self-Charging Power Cloth. *Appl. Phys. Lett.* **2017**, *111*, 073901.
- (25) Liu, M.; Cong, Z.; Pu, X.; Guo, W.; Liu, T.; Li, M.; Zhang, Y.; Hu, W.; Wang, Z. L. High-Energy Asymmetric Supercapacitor Yarns for Self-Charging Power Textiles. *Adv. Funct. Mater.* **2019**, *29*, 1806298.
- (26) He, T.; Sun, Z.; Shi, Q.; Zhu, M.; Anaya, D. V.; Xu, M.; Chen, T.; Yuce, M. R.; Thean, A. V.-Y.; Lee, C. Self-Powered Glove-Based Intuitive Interface for Diversified Control Applications in Real/Cyber Space. *Nano Energy* **2019**, *58*, 641–651.
- (27) Pu, X.; Song, W.; Liu, M.; Sun, C.; Du, C.; Jiang, C.; Huang, X.; Zou, D.; Hu, W.; Wang, Z. L. Wearable Power-Textiles by Integrating Fabric Triboelectric Nanogenerators and Fiber-Shaped Dye-Sensitized Solar Cells. *Adv. Energy Mater.* **2016**, *6*, 1601048.
- (28) Hu, L.; Pasta, M.; Mantia, F. L.; Cui, L.; Jeong, S.; Deshazer, H. D.; Choi, J. W.; Han, S. M.; Cui, Y. Stretchable, Porous, and Conductive Energy Textiles. *Nano Lett.* **2010**, *10*, 708–714.
- (29) Liu, Z.; Wu, Z. S.; Yang, S.; Dong, R.; Feng, X.; Mullen, K. Ultraflexible In-Plane Micro-Supercapacitors by Direct Printing of Solution-Processable Electrochemically Exfoliated Graphene. *Adv. Mater.* **2016**, *28*, 2217–2222.
- (30) Chen, Y.; Li, X.; Bi, Z.; Li, G.; He, X.; Gao, X. Stamp-Assisted Printing of Nanotextured Electrodes for High-Performance Flexible Planar Micro-Supercapacitors. *Chem. Eng. J.* **2018**, *353*, 499–506.
- (31) Kwak, S. S.; Kim, H.; Seung, W.; Kim, J.; Hinchet, R.; Kim, S. W. Fully Stretchable Textile Triboelectric Nanogenerator with Knitted Fabric Structures. *ACS Nano* **2017**, *11*, 10733–10741.
- (32) Kim, K. N.; Chun, J.; Kim, J. W.; Lee, K. Y.; Park, J.-U.; Kim, S.-W.; Wang, Z. L.; Baik, J. M. Highly Stretchable 2D Fabrics for Wearable Triboelectric Nanogenerator under Harsh Environments. *ACS Nano* **2015**, *9*, 6394–6400.
- (33) Lai, Y.-C.; Deng, J.; Zhang, S. L.; Niu, S.; Guo, H.; Wang, Z. L. Single-Thread-Based Wearable and Highly Stretchable Triboelectric Nanogenerators and Their Applications in Cloth-Based Self-Powered

Human-Interactive and Biomedical Sensing. *Adv. Funct. Mater.* **2017**, *27*, 1604462.

(34) Zhu, M.; Huang, Y.; Ng, W. S.; Liu, J.; Wang, Z.; Wang, Z.; Hu, H.; Zhi, C. 3D Spacer Fabric Based Multifunctional Triboelectric Nanogenerator with Great Feasibility for Mechanized Large-Scale Production. *Nano Energy* **2016**, *27*, 439–446.

(35) Wang, Z.; Ruan, Z.; Ng, W. S.; Li, H.; Tang, Z.; Liu, Z.; Wang, Y.; Hu, H.; Zhi, C. Integrating a Triboelectric Nanogenerator and a Zinc-Ion Battery on a Designed Flexible 3D Spacer Fabric. *Small Methods* **2018**, *2*, 1800150.

(36) Yu, X.; Su, X.; Yan, K.; Hu, H.; Peng, M.; Cai, X.; Zou, D. Stretchable, Conductive, and Stable PEDOT-Modified Textiles through a Novel *In Situ* Polymerization Process for Stretchable Supercapacitors. *Adv. Mater. Technol.* **2016**, *1*, 1600009.

(37) Zheng, Y.; Yang, Y.; Chen, S.; Yuan, Q. Smart, Stretchable and Wearable Supercapacitors: Prospects and Challenges. *CrystEngComm* **2016**, *18*, 4218–4235.

(38) Xu, P.; Gu, T.; Cao, Z.; Wei, B.; Yu, J.; Li, F.; Byun, J.-H.; Lu, W.; Li, Q.; Chou, T.-W. Carbon Nanotube Fiber Based Stretchable Wire-Shaped Supercapacitors. *Adv. Energy Mater.* **2014**, *4*, 1300759.

(39) Chen, T.; Hao, R.; Peng, H.; Dai, L. High-Performance, Stretchable, Wire-Shaped Supercapacitors. *Sci. Rep.* **2015**, *4*, 618–622.

(40) Yang, Q.; Cui, S.; Ge, Y.; Tang, Z.; Liu, Z.; Li, H.; Li, N.; Zhang, H.; Liang, J.; Zhi, C. Porous Single-Crystal $\text{NaTi}_2(\text{PO}_4)_3$ via Liquid Transformation of TiO_2 Nanosheets for Flexible Aqueous Na-Ion Capacitor. *Nano Energy* **2018**, *50*, 623–631.

(41) Dong, K.; Wang, Y. C.; Deng, J.; Dai, Y.; Zhang, S. L.; Zou, H.; Gu, B.; Sun, B.; Wang, Z. L. A Highly Stretchable and Washable All-Yarn-Based Self-Charging Knitting Power Textile Composed of Fiber Triboelectric Nanogenerators and Supercapacitors. *ACS Nano* **2017**, *11*, 9490–9499.

(42) Liu, M.; Pu, X.; Cong, Z.; Liu, Z.; Liu, T.; Chen, Y.; Fu, J.; Hu, W.; Wang, Z. L. Resist-Dyed Textile Alkaline Zn Microbatteries with Significantly Suppressed Zn Dendrite Growth. *ACS Appl. Mater. Interfaces* **2019**, *11*, 5095–5106.

(43) Yang, Z.; Pang, Y.; Han, X. L.; Yang, Y.; Ling, J.; Jian, M.; Zhang, Y.; Yang, Y.; Ren, T. L. Graphene Textile Strain Sensor with Negative Resistance Variation for Human Motion Detection. *ACS Nano* **2018**, *12*, 9134–9141.

(44) Gaikwad, A. M.; Zamarayeva, A. M.; Rousseau, J.; Chu, H.; Derin, I.; Steingart, D. A. Highly Stretchable Alkaline Batteries Based on an Embedded Conductive Fabric. *Adv. Mater.* **2012**, *24*, 5071–5076.

(45) Wang, C.; Zhang, M.; Xia, K.; Gong, X.; Wang, H.; Yin, Z.; Guan, B.; Zhang, Y. Intrinsically Stretchable and Conductive Textile by a Scalable Process for Elastic Wearable Electronics. *ACS Appl. Mater. Interfaces* **2017**, *9*, 13331–13338.

(46) Yue, B.; Wang, C.; Ding, X.; Wallace, G. G. Polypyrrole Coated Nylon Lycra Fabric as Stretchable Electrode for Supercapacitor Applications. *Electrochim. Acta* **2012**, *68*, 18–24.

(47) Yang, N.; Xu, X.; Li, L.; Na, H.; Wang, H.; Wang, X.; Xing, F.; Gao, J. A Facile Method to Prepare Reduced Graphene Oxide with Nano-Porous Structure as Electrode Material for High Performance Capacitor. *RSC Adv.* **2016**, *6*, 42435–42442.

(48) Kudin, K. N.; Ozbas, B.; Schniepp, H. C.; Prud'homme, R. K.; Aksay, I. A.; Car, R. Raman Spectra of Graphite Oxide and Functionalized Graphene Sheets. *Nano Lett.* **2008**, *8*, 36–41.

(49) Chen, X.; Lin, H.; Chen, P.; Guan, G.; Deng, J.; Peng, H. Smart, Stretchable Supercapacitors. *Adv. Mater.* **2014**, *26*, 4444–4449.

(50) Yong, S.; Owen, J.; Beeby, S. Solid-State Supercapacitor Fabricated in a Single Woven Textile Layer for E-Textiles Applications. *Adv. Eng. Mater.* **2018**, *20*, 1700860.

(51) Guo, R.; Chen, J.; Yang, B.; Liu, L.; Su, L.; Shen, B.; Yan, X. In-Plane Micro-Supercapacitors for an Integrated Device on One Piece of Paper. *Adv. Funct. Mater.* **2017**, *27*, 1702394.

(52) Kurra, N.; Ahmed, B.; Gogotsi, Y.; Alshareef, H. N. MXene-on-Paper Coplanar Microsupercapacitors. *Adv. Energy Mater.* **2016**, *6*, 1601372.

(53) Lv, J.; Jeerapan, I.; Tehrani, F.; Yin, L.; Silva-Lopez, C. A.; Jang, J.-H.; Joshua, D.; Shah, R.; Liang, Y.; Xie, L.; Soto, F.; Chuncai, Kong; Karshalev, E.; Chen, C.; Yang, Z.; Wang, J. Sweat-Based Wearable Energy Harvesting-Storage Hybrid Textile Devices. *Energy Environ. Sci.* **2018**, *11*, 3431–3442.

(54) Kim, D.; Keum, K.; Lee, G.; Kim, D.; Lee, S.-S.; Ha, J. S. Flexible, Water-Proof, Wire-Type Supercapacitors Integrated with Wire-Type UV/NO₂ Sensors on Textiles. *Nano Energy* **2017**, *35*, 199–206.

(55) Jiang, Q.; Kurra, N.; Alhabeab, M.; Gogotsi, Y.; Alshareef, H. N. All Pseudocapacitive MXene-RuO₂ Asymmetric Supercapacitors. *Adv. Energy Mater.* **2018**, *8*, 1703043.

(56) Yang, Q.; Huang, Z.; Li, X.; Liu, Z.; Li, H.; Liang, G.; Wang, D.; Huang, Q.; Zhang, S.; Chen, S.; Zhi, C. A Wholly Degradable, Rechargeable Zn-Ti₃C₂ MXene Capacitor with Superior Anti-Self-Discharge Function. *ACS Nano* **2019**, *13*, 8275–8283.

(57) Cheng, X.; Pan, J.; Zhao, Y.; Liao, M.; Peng, H. Gel Polymer Electrolytes for Electrochemical Energy Storage. *Adv. Energy Mater.* **2018**, *8*, 1702184.

(58) Nguyen, V.; Zhu, R.; Yang, R. Environmental Effects on Nanogenerators. *Nano Energy* **2015**, *14*, 49–61.

(59) Shen, J.; Li, Z.; Yu, J.; Ding, B. Humidity-Resisting Triboelectric Nanogenerator for High Performance Biomechanical Energy Harvesting. *Nano Energy* **2017**, *40*, 282–288.

(60) Li, L.; Fu, C.; Lou, Z.; Chen, S.; Han, W.; Jiang, K.; Chen, D.; Shen, G. Flexible Planar Concentric Circular Micro-Supercapacitor Arrays for Wearable Gas Sensing Application. *Nano Energy* **2017**, *41*, 261–268.

(61) Pu, X.; Liu, M.; Li, L.; Han, S.; Li, X.; Jiang, C.; Du, C.; Luo, J.; Hu, W.; Wang, Z. L. Wearable Textile-Based In-Plane Micro-supercapacitors. *Adv. Energy Mater.* **2016**, *6*, 1601254.

(62) Raj, C. J.; Kim, B. C.; Cho, W. J.; Lee, W. G.; Jung, S. D.; Kim, Y. H.; Park, S. Y.; Yu, K. H. Highly Flexible and Planar Supercapacitors Using Graphite Flakes/Polypyrrole in Polymer Lapping Film. *ACS Appl. Mater. Interfaces* **2015**, *7*, 13405–13414.

(63) Meng, Q.; Wang, K.; Guo, W.; Fang, J.; Wei, Z.; She, X. Thread-Like Supercapacitors Based on One-Step Spun Nano-composite Yarns. *Small* **2014**, *10*, 3187–3193.